JARQ 28, 79-89 (1994)

Seasonal Changes of Albedo and Micrometeorological Conditions of Vegetation in a Semi-Arid Area in Inner Mongolia, China

Yoshinobu HARAZONO*, Schenggong LI and Jianyou SHEN****

* Department of Environmental Resources, National Institute of Agro-Environmental Sciences (Tsukuba, Ibaraki, 305 Japan)
** The Institute of Desert Research, Academia Sinica (Lanzhou, China, 730000)

Abstract

Field observations were carried out in grasslands in a semi-arid area in China in order to analyze the mechanism of desertification, and the micrometeorological characteristics were examined in relation to desertification. Additional measurements were carried out over a dune and a vegetated area for comparison. Albedo values over the grassland which changed with grass growth, were significantly different from those at the humid vegetation site. The values were higher when the amount of grass was small, and changed with the surface conditions of dry soil and vegetation. Wind profile over the grass showed a logarithmic curve during the measurement periods, while that over the dune in the daytime was similar to a turbulent mixing layer, which prevented plant growth. Evapotranspiration of the grassland *ET* was 2.8 mm/day in early August, while it was less than 1 mm/day in the dry season. The heat budget of the grassland undergoing desertification was close to that of the dune.

Discipline: Agro-meteorology/Agricultural environment
Additional key words: dune, heat budget, grassland, wind profile

Introduction

Most grasslands in the semi-arid areas are currently undergoing desertification which has been brought about not only by the climatic change but also by human activities such as overgrazing and poor field management[1]. As desertification is an important environmental problem on a global scale[10], a comprehensive investigation to analyze the mechanism involved in the desertification of semi-arid ecosystems is required. Although studies on desert climate and changes of land uses have been reported, most of them were carried out in the Sahel, North-Central Africa, and in Australia[2-4]. The actual conditions of desertification and the characteristics of barren lands were investigated in China using remote sensing techniques[11,12]. However, information on the micrometeorological conditions of a plant community which is undergoing desertification, especially in the semi-arid areas in China is limited.

This study focused on the role of the micrometeorology in a plant community in the mechanism of desertification in semi-arid areas. A plant community has its own specific ecosystem, and progression of desertification

destroys its micrometeorological characteristics related to growth leading to an irreversible decay of the plant community. In this study, the micrometeorological conditions within and above the plant community were examined in relation to desertification through field measurements in a semi-arid area in China. The field observations were carried out from October 1990, in the framework of a cooperative study between Japan and China, in accordance with the Japan–China joint study project sponsored by the Science and Technology Agency, Japan.

Location and method of measurements

1) Analysis of climatic conditions of the measurement sites

Field measurements were carried out at Naiman (N 42°58′, E 120°43′, 363 m above sea level), located in the southeastern part of Korqin Sandy Land, Northeast China, under a semi-arid climate. Geomorphological landscape in this region is characterized by dunes alternating with gently undulating lowland areas where farmland and a few residential patches are distributed. The sandy soil contains mostly coarse sand and silt.

The annual solar radiation amounts to 5,210 MJ/m^2, and the total annual sunshine duration is 2,950 hr. Table 1 shows the average air temperatures (mean, minimum, and maximum), precipitation, and evaporation recorded over a 10-year period (1979–1988). The monthly average air temperature is −13.1°C in January and 23.7°C in July, respectively. The frostless period is in the range of 137–150 days a year. The annual precipitation is about 370 mm, with more than 65% of which falling during June and August. The annual evaporation is around 1,740 mm. Monthly evaporation reaches high levels in April, May and June, although the solar radiation levels in these months are lower than those in July and August, and the daily evaporation during April and June exceeds the daily net radiation. Northwest wind prevails in winter and spring, and southwest to south wind in summer and autumn. The mean annual wind speed is 3.5–4.1 m/s, but in winter and spring frequent gales whose wind speeds are higher than 20 m/s occur. Dry and strong winds in winter and

Table 1. Monthly average (1979–1988) of mean air temperature, maximum air temperature, minimum air temperature, precipitation, and evaporation (Naiman, semi-arid area, Inner Mongolia, China)

		Month						
		1	2	3	4	5	6	7
Mean temp.	(°C)	−12.6	−9.7	−1.6	8.5	16.4	21.4	23.7
Max. temp.	(°C)	−6.3	−3.3	5.2	15.1	23.1	27.5	29.1
Min. temp.	(°C)	−17.3	−14.8	−7.3	2.5	10.0	15.6	18.9
Precipitation	(mm)	0.57	2.03	7.11	20.89	32.56	69.39	99.79
Evaporation	(mm)	30.5	42.6	104.6	208.5	287.0	260.7	220.1

		Month					Average	Total
		8	9	10	11	12		
Mean temp.	(°C)	22.1	15.8	7.9	−2.3	−9.4	6.7	
Max. temp.	(°C)	27.5	22.2	14.6	4.0	−3.3	12.9	
Min. temp.	(°C)	17.5	10.2	2.4	−7.0	−13.7	1.4	
Precipitation	(mm)	77.42	40.35	12.33	4.74	3.39	30.9	370.6
Evaporation	(mm)	189.7	163.7	131.5	67.6	33.8	145.0	1740.3

spring lead to a high evaporation rate through the exchange between sensible heat and latent heat, and eventually evaporation exceeds net radiation.

Air temperature in winter is too low for plant growth and a high level of potential evapotranspiration prevents the growth and development of plants in the spring and beginning of summer, which is responsible for desertification in the eastern part of Inner Mongolia.

2) Characteristics of measurement sites

We selected four different measurement sites, a sand dune, a humid vegetation site, a grassland for sheep grazing, and farmland with a soybean field. The sand dune was covered almost completely with sand which drifted easily by strong wind and the vegetation was scant (vegetation index *VI* was less than 5%). The humid vegetation site was located in inter-dune lowland areas with plenty of soil water. As a result, a vegetation consisting of several species of weeds grew to stands of about 1 m. The grassland was located around the dune and grass grew after May. The farmland was located around residential patches and was irrigated almost every two weeks.

3) Methods and instruments for measurement

Field measurements of heat budget and wind profiles using a pole 6 m in height were carried out over the grassland, and measurements over the dune and the vegetation were also carried out for comparison. Each site provided a sufficient fetch. The parameters determined at respective heights in 1991 are listed in Table 2.

The equipment used in China was calibrated at the Institute of Agro-Environmental Sciences before set up at each site, and each calibration formula of the equipment was used in data analysis. Cup anemometers and a wind vane (Makino, AF750, VF16) were used for the measurement of the wind profiles up to a 5.8 m height and the wind direction, respectively. Gradients of air temperature were obtained from the measurements at two heights using ventilated psychrometers with thermocouple sensors (Type T) or platinum resistance thermometers and those of humidity were obtained using electrostatic capacity humidity sensors at two heights. Net radiation, solar radiation and its reflection were measured with a radiometer (Eko, CN11) and pyranometer (Iio, SR2), respectively. Soil temperature and soil heat flux were also measured with platinum resistance thermometers and heat flow plates (Eko, CN9), respectively.

Data were sampled every 2 min using a data

Table 2. Parameters determined at respective heights

Parameters	Height (m)			
	Sand dune	Dry grassland	Soybean field	Humid vegetation site
Net radiation	1.2	1.2	1.2	1.2
Solar radiation (Rs)	1.2	1.3	1.3	1.3
Reflected Rs	0.9	1.0	1.0	0.9
Soil heat flux	1, 5 cm	1, 5 cm	1, 5 cm	1, 5 cm
Air temperature	0.2, 2.5	0.3, 2.5	0.6, 2.8	1.4, 3.1
Relative humidity	0.2, 2.5	0.3, 2.5	0.6, 2.8	1.4, 3.1
Soil temperature	1, 5, 10, 20, 50 cm	1, 5, 10, 20, 50 cm	1, 5, 10, 20, 50 cm	1, 5, 10, 20, 40 cm
Wind direction	5.0	5.0	5.3	5.8
Wind speed	0.2, 0.6, 1.2, 2.5, 5.0	0.3, 0.6, 1.2, 2.5, 5.0	0.6, 1.1, 1.8, 2.8, 5.3	0.9, 1.4, 2.1, 3.1, 5.8

logger (North Hightech, IDL3200) at the measurement sites, then averaged every 10 min using a personal computer (Epson, 286L) in the laboratory. Each set of measurements was continued for almost 3 days at a site. A portable power generator (Honda, EB300EX) was used for power supply.

4) Method of analysis

In order to investigate the micrometeorological conditions, heat budget and water budget, the energy budget method and the aerodynamic method were applied for evaluating the fluxes. The outline of both methods used in the present study is as follows.

(1) Energy budget analysis

The heat budget over a surface is given by the equation:

$$Rn + H + lE + G = 0 \cdots\cdots (1)$$

where Rn, H, and lE are the net radiation, sensible heat flux, and latent heat flux (l is the latent heat of vaporization of liquid water and E is the evaporation rate), and G is the heat flux through the soil surface (W/m^2). Rn and G can be measured directly using proper sensors. We define Bowen ratio β by the following equation, where γ is the thermodynamic value of the psychometric constant, T_{a1}, T_{a2} and e_1, e_2 are air temperatures at two levels and corresponding water vapor pressures, respectively.

$$\beta = \frac{H}{lE} = \gamma \frac{\partial T}{\partial e} = \gamma \frac{T_{a1} - T_{a2}}{e_1 - e_2} \cdots (2)$$

H and lE are calculated using air temperature and water vapor pressure, and Rn and G as follows.

$$H = (Rn - G)/(1 + \beta^{-1}) \cdots\cdots (3)$$
$$lE = (Rn - G)/(1 + \beta) \cdots\cdots (4)$$

(2) Aerodynamic approach

In the boundary layer, the wind profile over the vegetation or the ground surface in the neutral condition can be expressed by formula (5)[9].

$$u(z) = \frac{u^*}{\varkappa} \ln \frac{z - d}{z_0} \cdots\cdots (5)$$

where u is the average wind speed at any height z, u^* is the friction velocity, $\varkappa$ is the von Karman's constant (0.40), d and z_0 are zero plane displacement and roughness length of the surface. u^*, d, and z_0 were calculated by the linear regression method of formulas (6) to (8) for every 10 min average data when the wind profiles showed a logarithmic curve[6].

$$\ln(z - d) = a\, u(z) + b \cdots\cdots (6)$$
$$u^* = \varkappa / a \cdots\cdots (7)$$
$$z_0 = \exp(b) \cdots\cdots (8)$$

The diffusion velocity Df was obtained from formula (9), although, when the atmospheric stability was not neutral, according to Thom[9], Df was corrected using the specific function $F(Ri)$ of the Richardson Number Ri, in formula (10). T_{a1}, T_{a2}, u_1 and u_2 are the air temperature and wind speed at the height of z_1 and z_2, respectively.

$$Df = F(Ri)\varkappa^2 \frac{(u_1 - u_2)}{\left(\ln \frac{z_1 - d}{z_2 - d}\right)^2} \cdots\cdots (9)$$

$$Ri = \frac{g}{T} \frac{(T_{a1} - T_{a2})(z_1 - z_2)}{(u_1 - u_2)^2} \cdots\cdots (10)$$

$$F(Ri) = (1 - 16Ri)^{0.75} \qquad -0.2 < Ri < 0 \cdots\cdots (11)$$

Sensible heat flux and latent heat flux were obtained by the product of Df and the differences in air temperature and humidity, dT and de, between heights z_1 and z_2.

$$H = \rho Cp\ dT\ Df \cdots\cdots (12)$$
$$lE = l\,de\,Df \cdots\cdots (13)$$

in which, ρ and Cp are the density and specific heat of air at a constant pressure.

(3) Adaptation of each method

As the atmospheric conditions were markedly different between daytime and night time,

both methods were required for the evaluation of diffusion velocities. The aerodynamic (gradient) method was mainly used for the evaluation of the nocturnal flux variations of H and lE, whereas the heat budget method for the diurnal variations.

Results and discussion

1) Differences in albedo values at several sites

Fig. 1 shows the daily variations of solar radiation, reflected solar radiation, and albedo values Ad over the dune, grassland, and the humid vegetation sites recorded during the mid-rainy season in 1991. Under almost identical clear conditions, the albedo value at noon was nearly 34% at the dune site, which was higher than that at the grassland site (19%) and the humid vegetation site (14%). The higher value was caused by the large proportion of solar radiation reflected at the dry sand surface, which was different from that of normal soil surface in humid zones. The minimum value of Ad within daily variations was recorded at noon for every site and the daily variation was greater at the humid vegetation site. As leaves, stems and some shoots are distributed from the bottom to the top of the plant vegetation, the reflection from the canopy changed with the sunlight incidence angle, hence affecting the albedo values.

2) Seasonal changes of albedo values over the grassland

Fig. 2 shows the seasonal changes of albedo values Ad over the grassland. The value of Ad at noon which was 0.25 in mid-May decreased to 0.20. The biomass of the grassland in mid-May was so low that the daily variation of the Ad values was similar to that over the dune, and then the Ad values decreased with the growth of grass. After June, since the biomass of grass did not increase appreciably due to sheep grazing, the Ad value at noon remained constant until September.

Seasonal changes of the Ad values and differences with the land surface conditions are caused by the conditions of the plant canopy (biomass and its activity) in semi-arid areas, which reflect the differences in heat and water budget of grassland and soil water contents. Thus, the albedo data can be used for remote sensing analysis to evaluate the vegetation growth and soil water conditions, although the Ad values changed within a day and seasonally in areas undergoing desertification as indicated

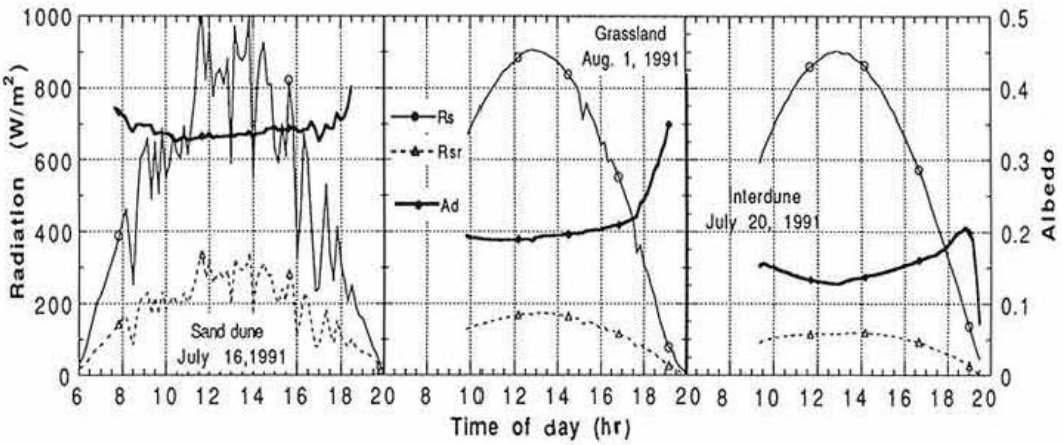

Fig. 1. Daily variations of solar radiation (thin line), reflected solar radiation (dotted line), and albedo Ad (thick line) values over dune, grassland, and humid vegetation sites in a semi-arid area in Inner Mongolia, China obtained during the mid-rainy season in 1991

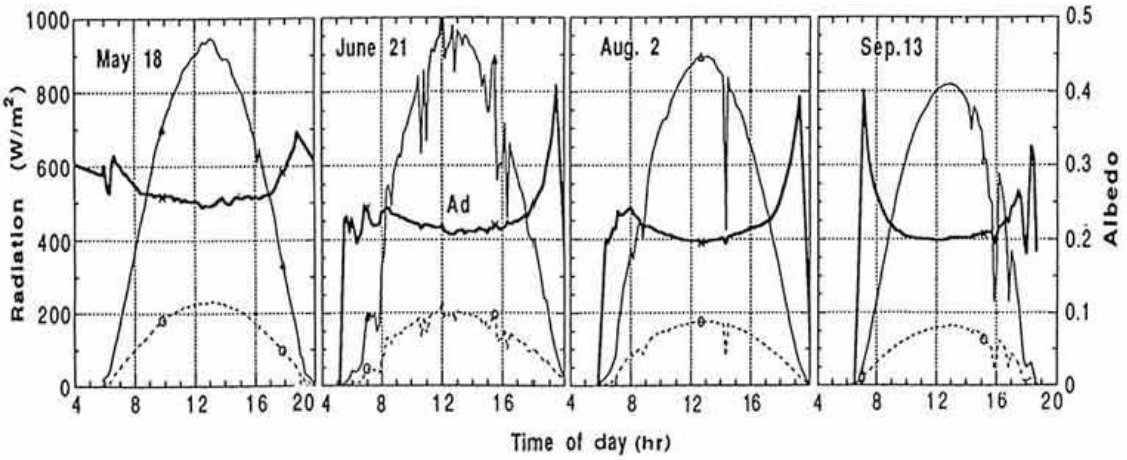

Fig. 2. Seasonal changes of albedo over the grassland in Inner Mongolia
Line designation is the same as in Fig. 1.

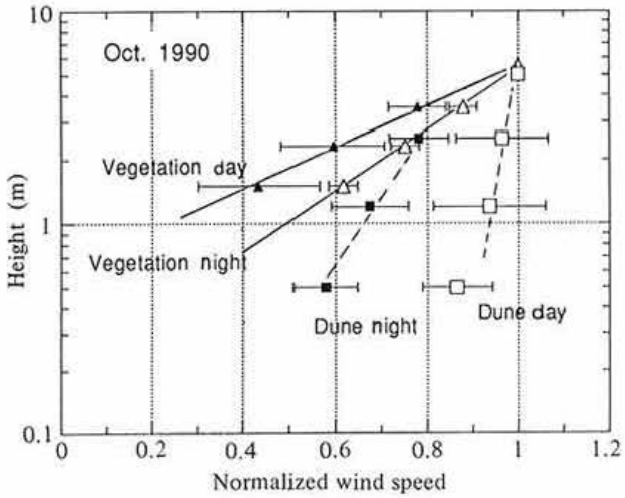

Fig. 3. Normalized wind profiles over the humid vegetation and the dune for daytime and night time in autumn

above. Albedo data obtained in the semi-arid areas show that one should be careful when using *Ad* values for remote sensing analysis.

3) Characteristics of wind profiles near the ground in semi-arid areas

Fig. 3 shows normalized logarithmic wind profiles over the humid vegetation site and the sand dune in the daytime and night time. The wind profiles over the grassland showed an almost linear curve (logarithmic) all day long, while those over the dune were not linear but similar to the profiles in a turbulent mixing layer in the daytime and a stable layer in the night time. The inclination of the logarithmic wind profile was inversely proportional to the friction stress (equivalent to friction velocity u^* from equations (6) and (7)), which was large

at the vegetation site, while very small at the dune site[5]. On the other hand, the wind speed just above the ground surface of the dune was very high, resulting in strong wind pressure on the few plants present and sand grains on the ground surface, leading to sand drift and inhibition of plant growth[7].

The friction stress increased with grass growth from May to September[8], which indicates that the biomass of vegetation was subjected to wind stress. Therefore, once grasslands in semi-arid areas are destroyed, the changes in the wind profile affect the micrometeorological conditions, which prevents the recovery of grass. Therefore a method of control of the wind profile using a kind of windbreak is recommended to promote the recovery and maintenance of the vegetation in semi-arid dune areas.

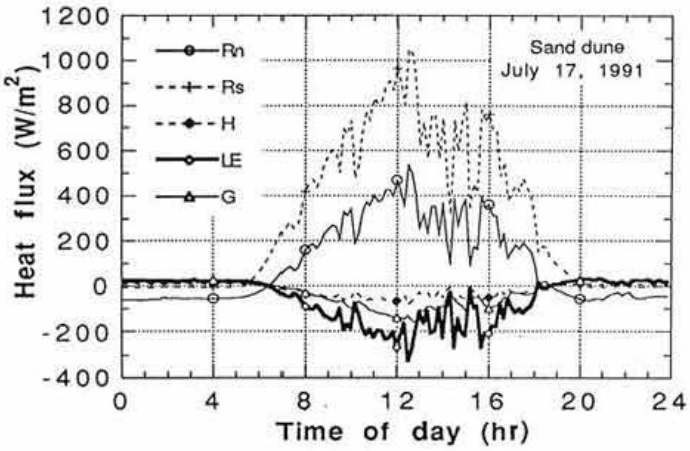

Fig. 4. Daily variations of heat budget components over the dune obtained in the rainy season in 1991
Symbols *Rn*, *Rs*, *H*, *lE*, and *G* represent net radiation, solar radiation, sensible heat flux, latent heat flux, and soil heat flux, respectively.

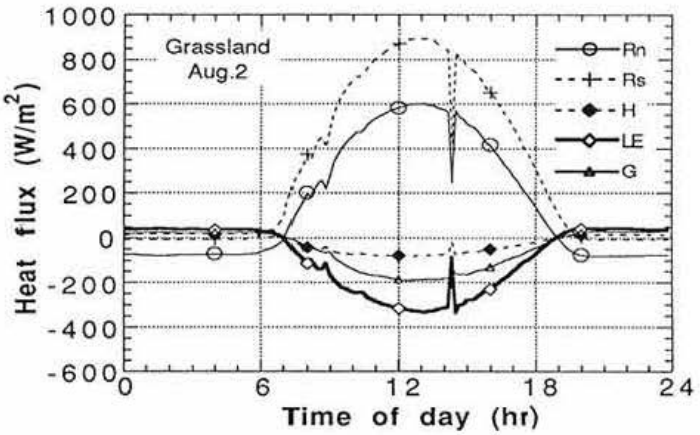

Fig. 5. Same as Fig. 4 for the grassland

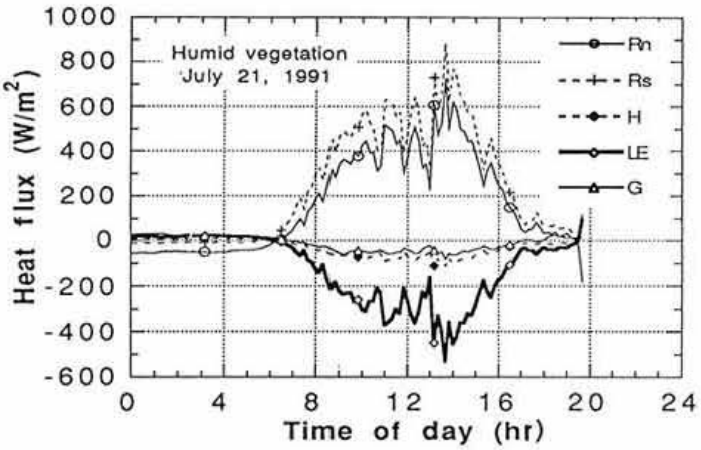

Fig. 6. Same as Fig. 4 for the humid vegetation with several species of weeds

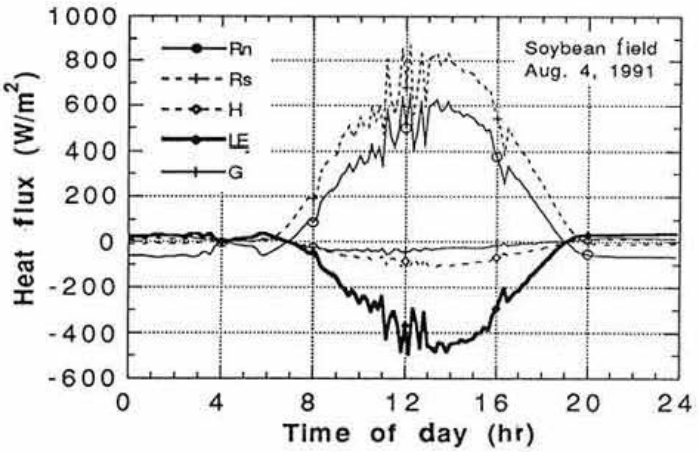

Fig. 7. Same as Fig. 4 for the soybean field which was irrigated almost every 2 weeks

4) Differences in heat budget components at the sites

Daily variations of the heat budget components in summer are shown in Fig. 4 for the dune, in Fig. 5 for the grassland, in Fig. 6 for the humid vegetation site, in Fig. 7 for the soybean field, respectively. Each figure includes solar radiation *Rs*, net radiation *Rn*, latent heat flux *lE*, sensible heat flux *H*, and heat flux at the ground surface *G*.

As the above results were obtained in the rainy season of 1991 when there was some precipitation, we measured the upward latent heat flux at the dune site in the daytime on a clear day, while in autumn the downward flux was obtained[7]. At the dune site, as the ratio of *Rn* to *Rs* was smaller than 0.5 and smallest within the sites, the absolute level of *lE* was low. At the humid vegetation and irrigated soybean field sites, as the latent heat flux *lE* was higher and the soil heat flux *G* was smaller compared to the other sites, the major part of

Table 3. Seasonal changes of heat budget components (MJ/m^2) in the daytime and contribution to net radiation (relative values) over the grassland in 1991

	(MJ/m^2)				Relative value		
	Rn	*H*	*lE*	*G*	*H/Rn*	*lE/Rn*	*G/Rn*
May 17	8.44	-1.51	-4.22	-2.71	0.18	0.50	0.32
June 21	10.31	-2.10	-5.75	-2.46	0.20	0.56	0.24
Aug. 2	15.91	-4.06	-6.95	-4.90	0.26	0.44	0.31
Aug.19	9.55	-4.54	-2.77	-2.24	0.48	0.29	0.23
Sep. 13	9.19	-4.90	+2.48	-1.81	0.53	0.27	0.20

energy was used for evapotranspiration of plants growing actively. At the grassland site, since the ratio *Rn/Rs* was almost two-thirds of that of the vegetation site, most of which was used as *lE* and *G*, the contribution of *H* was small.

In this season, it was interesting to note that the contribution of *H* was small in the semi-arid area, while *lE* was dominant over the plant canopy when there was plenty of water and *G* contributed significantly at the dune and the dry grassland sites where water availability was limited.

5) Seasonal changes in heat budget at the grassland site

Seasonal changes in the heat budget at the grassland site were examined. Diurnal maximum levels of net radiation *Rn* at the grassland were 500 W/m^2 in May and September, and more than 600 W/m^2 in mid-June and August. Most of *Rn* was used for evapotranspiration, and the maximum latent heat flux *lE* was 350 W/m^2 in mid-June, which is equivalent to 0.5 mm/hr of evapotranspiration. After mid-August the dry season started and there was very little precipitation. In September, *lE* in the morning over the dry grassland was almost at the same level as that in the rainy season, while in the afternoon the value decreased rapidly and the value of sensible heat flux *H* increased, which reflected the limiting soil water contents for evapotranspiration at the grassland site in the dry season[8].

Table 3 shows the seasonal changes in the daily heat budget components over the grassland and the contribution to the net radiation. The contribution of *lE* was highest in June, and decreased with grass growth and maturation. The maximum daily value of *lE* was approximately 7 MJ/m^2, equivalent evapotranspiration was 2.8 mm in early August, at the end of the rainy season when the plant biomass level was at its maximum, while it was less than 1 mm in the dry season in mid-September. Table 3 shows that the evapotranspiration at the grassland site was independent of the atmospheric moisture deficit which was high in the dry season, and was dependent on the plant activity and the soil water level. The contribution of *G* was high in the first half of the season, which was caused by the sparse grass density and low soil temperature. On the other hand, the *H* value increased with the season in contrast to the decreases in *G* and *lE*, the contribution being particulary high in the dry season.

6) Contribution of accumulated heat budget components

The daily accumulated values of the heat budget components of the dune, humid vegetation site, grassland, and soybean field sites are given in Table 4 for clear days in the summer season. The contribution of the accumulated heat budget components varied considerably from site to site.

In the daytime, most of *Rn* was used as

Table 4. Differences in heat budget components (MJ/m^2) and contribution in summer season (1991) among four different sites in semi-arid areas in China

Time	Site	*Rn*	*H*(*H*/*Rn*)	*lE*(*lE*/*Rn*)	*G*(*G*/*Rn*)
Day	Sand dune	11.89	-2.50	-5.98	-3.41
		(100)	(-21)	(-50)	(-29)
	Dry grassland	16.73	-3.41	-9.35	-3.97
		(100)	(-20)	(-56)	(-24)
	Soybean field	14.40	-2.60	-10.86	-0.94
		(100)	(-18)	(-76)	(-6)
	Humid vegetation	21.06	-4.49	-13.46	-3.11
		(100)	(-21)	(-64)	(-15)
Night	Sand dune	-1.98	0.25	0.40	1.33
		(-100)	(13)	(20)	(67)
	Dry grassland	-2.51	0.44	0.88	1.19
		(-100)	(18)	(35)	(47)
	Soybean field	-1.88	0.36	0.92	0.60
		(-100)	(19)	(49)	(32)
	Humid vegetation	-2.57	0.43	0.74	1.40
		(-100)	(17)	(29)	(54)

evapotranspiration *lE* over the grassland, soybean field, and humid grassland, although the contribution of *lE* at the dune site was smaller and that of *G* was larger compared to those at sites with vegetation. In the irrigated soybean field, the contribution of *lE* accounted for more than three-fourths. It is interesting to note that the contribution of *H* was the smallest in the daytime for the dune and grassland even when the ground surface was dry, while that of *G* was the smallest for the vegetated sites.

At night, most of *Rn* was supported by *G* at each site, in particular, almost two-thirds of *Rn* was provided by *G* at the dune site. At night the contribution of *lE* to *Rn* was significant, especially in the irrigated soybean field *lE* accounted for almost half of *Rn*, due to the high level of evapotranspiration in the daytime. When it was windy and the atmospheric humidity was high, the contribution of *lE* to *Rn* increased at the dune site after the rain.

The ground surface temperature at the dune site changed rapidly just after sunrise and sunset, indicating that most of *Rn* was transformed into *G* in the morning and *G* compensated for upward *Rn* after sunset. These hourly variations of the heat budget seemed to be important in the partition of energy for the latent heat flux, which affects the mechanisms of desertification in semi-arid areas.

Conclusion

Significant micrometeorological characteristics were revealed by field measurements conducted in semi-arid areas in Inner Mongolia, through the cooperative joint study between the National Institute of Agro-Environmental Sciences and Institute of Desert Research, Academia Sinica, China, along the lines of the project sponsored by the Science and Technology Agency, Japan. The results are summarized as follows:

(1) Albedo value of the grassland decreased from 0.25 in mid-May to 0.2 after June, which reflected the surface conditions.

(2) Wind profile showed a logarithmic curve over grass and vegetation, while a turbulent mixing layer was dominant over the dune, which prevented plant growth.

(3) Maximum evapotranspiration *ET* was 2.8

mm/day in early August, while it was less than 1 mm/day in the dry season. *ET* was dependent on the plant and soil water conditions more than on the atmospheric water deficit conditions.

(4) The latent heat flux *lE* in semi-arid areas depended on the vegetation conditions and the soil available water content.

(5) The heat budget at the humid vegetation site and the irrigated farmland site was significantly different from that at the dry grassland and the dune sites.

References

1) Biswas, M. R. (1978): UN Conference on desertification, in prospect. *Environ. Conserv.*, **5**, 247-262.
2) Bunting, H. et al. (1976): Rainfall trends in west African Sahel. *Q. J. Roy. Soc.*, **120**, 59-64.
3) Charney, J. G. (1975): Dynamics of deserts and drought in the Sahel. *Q. J. Roy. Met. Soc.*, **101**, 193-202.
4) Costin, A. B. (1971): Vegetation, soils, and climate in late quaternary southeastern Australia. *In* Aboriginal man and environment in Australia. ed. Mulvaney, D. J., Australian National University Press, Canberra, 14-25.
5) Harazono, Y., Murakami, T. & Oikawa, T. (1990): The interaction of turbulent air flow and communities of rice plants and red-pine —Effects on fluxes and drag coefficients over canopies due to differences in canopy structure. *Bull. Environ. Res. Cent.* (Univ. of Tsukuba), **14**, 1-14 [In Japanese].
6) Harazono, Y., Yamada, C. & Nishizawa, T. (1992): Characteristics of aerodynamic parameters and turbulent transport of momentum and CO_2 over a soybean canopy. *Bull. Environ. Res. Cent.* (Univ. of Tsukuba), **16**, 1-14 [In Japanese].
7) Harazono, Y. et al. (1992): Micrometeorological characteristics of a sand dune in the eastern part of inner Mongolia, China in autumn. *J. Agric. Met.*, **47**, 217-224 [In Japanese with English summary].
8) Harazono, Y. et al. (1993): Seasonal micrometeorological changes over a grassland in inner Mongolia. *J. Agric. Met.*, **48**, 711-714.
9) Thom, A. S., (1975): Momentum, mass and heat exchange of plant communities. *In* Vegetation and atmosphere. ed. Monteith, J. L., Academic Press, London, 57-110.
10) Wolman, M. G. & Fournier, F. G. A. (eds.) (1987): Land transformation in agriculture. Scope 32, John Wiley, Sussex, pp.531.
11) Zhu, Z. (1986): Deserts in China. Institute of Desert Research, Academia Sinica, Lanzhou, pp.132.
12) Zhu, Z. (1988): Desertification and rehabilitation in China. The International Center for Education and Research on Desertification Control, Lanzhou, pp.222.

(Received for publication, Aug. 5, 1993)